[20] Y. Katanasaka, T. Ishii, T. Asai, H. Naitou, N. Maeda, F. Koizumi, S. Miyagawa, N. Ohashi, N. Oku, Cancer antineovascular therapy with liposome drug delivery systems targeted to BiP/GRP78, Int. J. Cancer 127 (2010) 2685–2698.
[21] M. Hamaoka, I. Chinen, T. Murata, S. Takashima, R. Iwamoto, E. Mekada, Anti-human HB-EGF monoclonal antibodies inhibiting ectodomain shedding of HB-EGF and diphtheria toxin binding, J. Biochem. 148 (2010) 55–69.
[22] T. Ishida, D.L. Iden, T.M. Allen, A combinatorial approach to producing terically stabilized (Stealth) immunoliposomal drugs, FEBS Lett. 460 (1999) 129–133.
[23] K. Goishi, S. Higashiyama, M. Klagsbrun, N. Nakano, T. Umata, M. Ishikawa, E. Mekada, N. Taniguchi, Phorbol ester induces the rapid processing of cell surface heparin-binding EGF-like growth factor: conversion from juxtacrine to paracrine growth factor activity, Mol. Biol. Cell 6 (1995) 967–980.
[24] K. Maruyama, N. Takahashi, T. Tagawa, K. Nagaike, M. Iwatsuru, Immunoliposomes bearing polyethyleneglycol-coupled Fab' fragment show prolonged circulation time and high extravasation into targeted solid tumors in vivo, FEBS Lett. 413 (1997) 177–180.
[25] C. Mamot, D.C. Drummond, U. Greiser, K. Hong, D.B. Kirpotin, J.D. Marks, J.W. Park, Epidermal growth factor receptor (EGFR)-targeted immunoliposomes mediate specific and efficient drug delivery to EGFR- and EGFRvIII-overexpressing tumor cells, Cancer Res. 63 (2003) 3154–3161.
[26] C. Mamot, D.C. Drummond, C.O. Noble, V. Kallab, Z. Guo, K. Hong, D.B. Kirpotin, J.W. Park, Epidermal growth factor receptor-targeted immunoliposomes significantly enhance the efficacy of multiple anticancer drugs in vivo, Cancer Res. 65 (2005) 11631–11638.
[27] N. Oku, Y. Tokudome, T. Asai, H. Tsukada, Evaluation of drug targeting strategies and liposomal trafficking, Curr. Pharm. Des. 6 (2000) 1669–1691.
[28] G. Haran, R. Cohen, L.K. Ba, Y. Barenholz, Transmembrane ammonium sulfate gradients in liposomes produce efficient and stable entrapment of amphipathic weak bases, Biochim. Biophys. Acta 1151 (1993) 201–215.
[29] N. Emanuel, E. Kedar, E.M. Bolotin, N.I. Smorodinsky, Y. Barenholz, Preparation and characterization of doxorubicin-loaded sterically stabilized immunoliposomes, Pharm. Res. 13 (1996) 352–359.

Journal of Controlled Release 181 (2014) 32–39

Contents lists available at ScienceDirect

Journal of Controlled Release

journal homepage: www.elsevier.com/locate/jconrel

Advanced cancer therapy by integrative antitumor actions *via* systemic administration of miR-499

Hidenori Ando [a], Tomohiro Asai [a], Hiroyuki Koide [a,b], Ayaka Okamoto [a], Noriyuki Maeda [c], Koji Tomita [c], Takehisa Dewa [d], Tetsuo Minamino [e], Naoto Oku [a,*]

[a] *Department of Medical Biochemistry, University of Shizuoka, School of Pharmaceutical Sciences, 52-1 Yada, Suruga-ku, Shizuoka 422-8526, Japan*
[b] *University of California Irvine, Irvine 92697, USA*
[c] *Nippon Fine Chemical Co. Ltd., 5-1-1 Umei, Takasago, Hyogo 676-0074, Japan*
[d] *Department of Life and Materials Engineering, Nagoya Institute of Technology, Gokiso-cho, Showa-ku, Nagoya 466-8555, Japan*
[e] *Department of Cardiovascular Medicine, Osaka University, Graduate School of Medicine, 2-2 Yamadaoka, Suita, Osaka 565-0871, Japan*

ARTICLE INFO

Article history:
Received 23 November 2013
Accepted 21 February 2014
Available online 2 March 2014

Keywords:
MicroRNA
miR-499
Cancer therapy
Gene delivery
Liposomes
Antiangiogenesis

ABSTRACT

Previously, we developed tetraethylenepentamine-based polycation liposomes (TEPA-PCL) as a vector for the delivery of small RNAs. In the present research, we attempted tumor-targeted delivery of miR-499 via systemic administration and evaluated the potency of this system as a therapeutic strategy to treat cancer. Lipoplexes were formed by mixing cholesterol-grafted miR-499 (miR-499-C) with TEPA-PCL. Firstly, human umbilical endothelial cells (HUVECs) and Colon 26 NL-17 mouse carcinoma cells were transfected with these lipoplexes in vitro. The results showed that miR-499 had antiangiogenic effects on the HUVECs and suppressed the secretion of vascular endothelial growth factor (VEGF) from the Colon 26 NL-17 cells. In addition, the growth of the latter cells was inhibited by transfection with miR-499-C/TEPA-PCL. For in vivo delivery of miR-499 to tumors via systemic injection, miR-499-C/TEPA-PCL were decorated with Ala-Pro-Arg-Pro-Gly (APRPG) peptide-conjugated polyethylene glycol (PEG) to prepare APRPG-PEG-modified lipoplexes carrying miR-499 (APRPG-miR-499). APRPG-miR-499 were injected into tumor-bearing mice via a tail vein, and these lipoplexes accumulated sufficiently in both angiogenic vessels and cancer cells. In addition, the expression of miR-499-target proteins and VEGF in the tumor cells was clearly suppressed by the treatment with APRPG-miR-499. Finally, the therapeutic effect of miR-499 on tumor growth was evaluated in mice. The tumor growth was significantly inhibited by the intravenous injection of APRPG-miR-499 at such a low dose as 0.5 mg/kg. These results suggest that miR-499 delivered by the present system has excellent potency to treat cancer via integrative anticancer actions.

1. Introduction

MicroRNAs (miRNAs) are expected to be novel therapeutic agents, especially for the treatment of cancer [1–6]. miRNAs possess partial complementarity to target mRNAs and thereby induce endogenous gene-silencing, resulting in the knockdown of the targeted series of proteins regulating specific signaling pathways multidirectionally. Therefore, miRNAs have attracted much attention as therapeutic molecules to treat certain kinds of cancers having genetic mutations.

In the treatment of cancer, the tumor microenvironment such as rule-out angiogenesis often affects the intratumoral distribution of certain nanoparticles after intravenous administration [7–10]. In addition, the hypoxic environment in the tumor might induce uncontrolled progression of the tumor [11]. Therefore, an appropriate therapeutic strategy is needed to improve the therapeutic effects of anti-cancer agents on tumor growth. In the present study, we focused on miR-499, one of the miRNAs that regulates specific signaling pathways especially under the conditions of hypoxia–ischemia [12]. miR-499 targets signaling pathways including those for calcineurin signaling and Wnt signaling [13], both of which are reported to be involved in angiogenesis. For example, calcineurin catalytic subunit α isoform (CnAα), one of the target molecules of miR-499, is related to the progression of angiogenesis *via* activation of the transcriptional factor referred to as nuclear factor of activated T cells (NFAT) [14,15]. It was also reported that this calcineurin/NFAT pathway regulates the activation of hypoxia-inducible factor 1-α (HIF1-α), resulting in the secretion of VEGF from cells [16]. In addition, VEGF is strongly regulated by the Wnt signaling pathway in certain cancer cells [17]. These reports suggest that suppression of these signaling pathways would have synergistic antiangiogenic effects *via* not only a direct effect on angiogenic endothelial cells but also inhibition of VEGF secretion from tumor cells. For effective cancer therapy, both angiogenic vessels and tumor cells should be damaged simultaneously [18]. miR-499 is considered to have the potential to carry out such dual therapy in light of the following findings: Inhibition of the calcineurin/NFAT pathway leads to positive modulation of certain cell-cycle

* Corresponding author. Tel.: +81 54 264 5701; fax: +81 54 264 5705.
E-mail address: oku@u-shizuoka-ken.ac.jp (N. Oku).

http://dx.doi.org/10.1016/j.jconrel.2014.02.019
0168-3659/

inhibitors and promotes caspase-dependent apoptosis [19]; calcineurin controls the mitogen-activated protein kinase (MAPK) signaling pathway [20]; and the activation of Wnt signaling promotes cell proliferation [21]. These reports suggest that miR-499 delivered into tumor cells would cause effective growth inhibition of tumors. Furthermore, targeting of calcineurin might be efficient, because increased expression of *DSCR1*, one of the over-expressed genes in patients with Down's syndrome and a negative regulator of VEGF–calcineurin signaling, confers significant suppression of tumor growth in mice [14]. Therefore, the tumor-targeted delivery of miR-499 into both angiogenic endothelial cells and tumor cells may be expected to have potential therapeutic effects on tumor growth *via* not only antiangiogenesis but also growth inhibition of tumor cells.

Previously, we developed tetraethylenepentamine-based polycation liposomes (TEPA-PCL) for the cytoplasmic delivery of small RNAs [22]. siRNA complexed with TEPA-PCL effectively causes gene-silencing *in vitro* [23], and has a significant therapeutic effect on tumor growth *in vivo via* systemic injection into tumor-bearing mice [24,25]. In addition, miR-92a, one of the miRNAs regulating the expression of certain proteins involved in angiogenesis, has an obvious silencing action and antiangiogenic effect *in vitro* when delivered *via* TEPA-PCL [26]. This effective induction of gene silencing by transfection with miR-92a lipoplexes is due to the potency of TEPA-PCL to deliver small RNAs into the cytoplasm functionally [27]. In the present research, we modified the surface of TEPA-PCL with polyethylene glycol (PEG)-conjugated Ala-Pro-Arg-Pro-Gly (APRPG) peptide (a ligand for angiogenic vessels) for systemic and tumor-targeted deliveries of miR-499, and evaluated the potential of miR-499 as a therapeutic agent to treat cancer *in vitro* and *in vivo*.

2. Material and methods

2.1. Preparation of TEPA-PCL and lipoplexes

Cholesterol-conjugated miR-499 (miR-499-C), carboxytetramethylrhodamine (TAMRA)-labeled miR-499-C (TAMRA-miR-499-C), and cholesterol-conjugated control miRNA (miCont-C) were purchased from Hokkaido System Science (Hokkaido, Japan). Cholesterol was conjugated to the 3′ end of the passenger strand of miRNAs, as previously reported [26,27]. miR-499 was composed of miR-499-5p and miR-499-3p (miR-499-5p: 5′-UUAAGACUUGCAGU GAUGUUU-3′, miR-499-3p: 5′-AACAUCACAGCAAGUCUGUGCU-3′). DCP-TEPA was synthesized as described previously [22]. Cholesterol, dipalmitoylphosphatidylcholine (DPPC), Ala-Pro-Arg-Pro-Gly (APRPG)-grafted polyethylene glycol (6000)-distearoylphosphatidylethanolamine (APRPG-PEG-DSPE), and polyethylene glycol (6000)-distearoylphosphatidylethanolamine (PEG-DSPE) were products from Nippon Fine Chemical (Hyogo, Japan). Dioleoylphosphatidylethanolamine (DOPE) was purchased from NOF (Tokyo, Japan).

For preparing TEPA-PCL, a lipid mixture containing DPPC, DOPE, cholesterol, and DCP-TEPA (3:4:4:1 as a molar ratio) was dissolved in *t*-butyl alcohol and lyophilized. TEPA-PCL were produced by hydration with RNase-free water. These liposomes were sized by extruding them 10 times through a polycarbonate membrane filter having a pore size of 100 nm (Nuclepore, Maidstone, UK). TEPA-PCL and miR-499-C were mixed in RNase-free water at a ratio of the nitrogen moiety derived from TEPA-PCL to the phosphorus from miR-499-C (N/P ratio) of 18 and incubated for 20 min at room temperature to form miR-499-C/TEPA-PCL lipoplexes. For systemic administration of miR-499, miR-499-C/TEPA-PCL were incubated with PEG-DSPE or APRPG-PEG-DSPE dissolved in RNase-free water at 50 °C for 20 min. Thus, PEG-modified miR-499-C/TEPA-PCL (PEG-miR-499) and APRPG-PEG-modified miR-499-C/TEPA-PCL (APRPG-miR-499) were prepared. The percent molar ratio of PEG-DSPE or APRPG-PEG-DSPE to total lipids was 10%. The size and ζ-potential of each sample were measured by using a Zetasizer Nano ZS (Malvern, Worcestershire, UK).

2.2. Transmission electron microscope (TEM)

TEPA-PCL, miR-499-C/TEPA-PCL or APRPG-miR-499 (0.5 mM as total lipid concentration) in a volume of 5 μL was placed on a grid (Nisshin EM, Tokyo, Japan) and dried-out by warm air. After performing this step for 3 cycles, each sample was negatively stained with 10 μL of 1 w/v ammonium molybdate for 1 min, and imaged with HT7700 TEM System (Hitachi High-Technologies, Tokyo, Japan). The images were recorded with a CCD camera at 1024 × 1024 pixels (Advanced Microscopy Techniques, Woburn, MA, USA).

2.3. Transfection of cells with miR-499 in vitro

Murine Colon 26 NL-17 carcinoma cells, established by Dr. Yamori (Japanese Foundation for Cancer Research, Tokyo, Japan), were kindly provided by Dr. Nakajima (SBI Pharmaceuticals, Tokyo, Japan). The cells were cultured in DME/Ham's F-12 medium (Wako, Osaka, Japan) supplemented with 10% fetal bovine serum (FBS, AusGeneX, Oxenford, Australia), 100 units/mL penicillin (MP Biomedicals, Irvine, CA, USA), and 100 μg/mL streptomycin (MP Biomedicals). Human umbilical vein endothelial cells (HUVECs) were purchased from Lonza (Walkersville, MD, USA) and cultured in endothelial cell growth medium-2 (EGM-2, Lonza).

Either the carcinoma or the endothelial cells were seeded onto culture plates and pre-incubated for 24 h at 37 °C. For transfection of cells, the culture medium was changed to fresh medium without antibiotics; and the cells were incubated with each lipoplex under the conditions of hypoxia (1% O_2, 94% N_2, and 5% CO_2) or normoxia (19% O_2, 76% N_2, 5% CO_2) for the selected time period as described for each experimental procedure.

2.4. Western blotting

Anti-CnAα rabbit polyclonal antibody (Cell Signaling Technology, Danvers, MA, USA), anti-frizzled family receptor 8 (FZD8) rabbit polyclonal antibody (Abcam, Cambridge, UK), anti-VEGF rabbit polyclonal antibody (Bioss, Woburn, MA, USA), and anti-β-actin rabbit polyclonal antibody (Sigma-Aldrich, St. Louis, MO, USA) were used for Western blotting, according to the manufacturer's instructions.

HUVECs (1.5×10^5 cells) or Colon 26 NL-17 cells (2.0×10^5 cells) were seeded onto 60-mm dishes and incubated with TEPA-PCL, miCont-C/TEPA-PCL or miR-499-C/TEPA-PCL at an miRNA concentration of 100 nM (300 pmol/3.0 mL/dish). Forty-eight hours after the start of transfection, cellular proteins were extracted with lysis solution composed of 0.1% Triton X-100 (Sigma-Aldrich), 0.15 M NaCl, 10 mM Tris–HCl (pH 7.4), 50 μg/mL aprotinin (Sigma-Aldrich), 200 μM leupeptin (Sigma-Aldrich), 2 mM phenylmethylsulfonyl fluoride (PMSF, Sigma-Aldrich), and 100 μM pepstatin A (Sigma-Aldrich). Total protein content was measured by using a BCA Protein Assay Reagent Kit (Pierce Biotechnology, Rockford, IL, USA). The cell extracts were subjected to 10% SDS-PAGE, separated by electrophoresis, and transferred electrophoretically onto an Immobilon®-P Transfer Membrane (Millipore, Billerica, MA, USA). After having been blocked with 3% bovine serum albumin (BSA, Sigma-Aldrich) in Tris–HCl-buffered saline containing 0.1% Tween 20 (Bio-Rad, Hercules, CA, USA) (TTBS, pH 7.4) for 1 h at room temperature, the membrane was incubated with a primary antibody (against CnAα, FZD8, VEGF or β-actin) overnight at 4 °C, and then with an HRP-conjugated secondary antibody for 1 h at room temperature. Each target-protein was visualized with a chemiluminescent substrate (ECL prime, GE Healthcare Bioscience, Buckinghamshire, UK), and analyzed with an LAS-3000 mini system (Fujifilm, Tokyo, Japan).

2.5. Tube formation assay

Matrigel™ (BD Biosciences, Bedford, MA, USA) was diluted to 4 mg/mL with EGM-2 without antibiotics, added to each well of a 24-well plate (0.2 mL/well), and allowed to undergo polymerization by a 30-min incubation at 37 °C. HUVECs (1.0×10^5 cells) were seeded onto a 60-mm dish and incubated with TEPA-PCL or miR-499-C/TEPA-PCL (100 nM; 300 pmol/3.0 mL/dish, or 200 nM; 600 pmol/3.0 mL/dish as miR-499) for 48 h. The transfected cells were then re-seeded onto the Matrigel™-coated wells (2.0×10^4 cells/well), incubated for 3.5 h for the formation of capillary tubes, and then observed under a microscope (Olympus IX71, Tokyo, Japan).

2.6. Growth inhibition assay

HUVECs (3.0×10^3 cells/well) or Colon 26 NL-17 cells (3.0×10^3 cells/well) were cultured in wells of a 96-well plate and incubated with miCont-C/TEPA-PCL or miR-499-C/TEPA-PCL (100 nM, 20 pmol/0.2 mL/well as miRNA) for 48 h. Then, the cell growth was evaluated by use of a Cell Counting Kit-8 (Dojindo, Kumamoto, Japan) in accordance with the manufacturer's instructions. Absorbance was measured with an Infinite® M200 (Tecan Group, Männedorf, Switzerland) at a test wavelength of 450 nm and a reference wavelength of 630 nm.

2.7. Evaluation of VEGF secretion from Colon 26 NL-17 cells

Colon 26 NL-17 cells (2.0×10^5 cells) were seeded onto a 60-mm dish and incubated with miCont-C/TEPA-PCL or miR-499-C/TEPA-PCL for 48 h. Conditioned medium in each group was collected, and the secreted VEGF was immunoprecipitated by use of a rabbit anti-VEGF antibody and a Dynabeads® Protein G Immunoprecipitation Kit (Life Technologies, Carlsbad, CA, USA). The beads were then denatured and subjected to SDS-PAGE followed by Western blotting with anti-VEGF antibody.

2.8. Experimental animals

Five-week-old BALB/c male mice were purchased from Japan SLC (Shizuoka, Japan). The animals were cared for according to the Animal Facility Guidelines of the University of Shizuoka. All animal experiments were approved by the Animal and Ethics Committee of the University of Shizuoka.

For preparation of tumor-bearing mice, Colon 26 NL-17 cells (1.0×10^6 cells/mouse) were implanted subcutaneously into the left posterior flank of BALB/c mice. Each lipoplex sample was administered *via* the tail vein at selected times after the implantation as described in each experiment.

2.9. Biodistribution of lipoplexes in the tumor-bearing mice after systemic administration

In order to label TEPA-PCL with a radioisotope, we added a trace amount of [^{3}H]cholesteryl hexadecyl ether (GE Healthcare) to the initial *t*-butyl alcohol solution and freeze-dried it with the component lipids of the TEPA-PCL. The tumor-bearing mice were injected with [^{3}H]-labeled TEPA-PCL, PEG-miR-499 or APRPG-miR-499 *via* a tail vein (74 kBq/mouse, 1.0 mg/kg as miR-499) on day 13 after the implantation. Twenty-four hours after the injection, these mice were sacrificed under deep anesthesia for collection of blood. The post-heparin plasma was obtained by centrifugation (5000 rpm, 10 min, 4 °C). Then, the heart, lungs, liver, spleen, kidneys, and the tumor were removed and weighed. Radioactivity in each organ was determined with a liquid scintillation counter (LSC-7400, Hitachi Aloka Medical, Tokyo, Japan). The total amount of the plasma was calculated based on the body weight of the mice, where the plasma volume was assumed to be 4.27% of the body weight based on the data for total blood volume [28].

2.10. Intratumoral distribution of miR-499 after the intravenous administration

The tumor-bearing mice were prepared and intravenously injected with TAMRA-miR-499-C formulated in APRPG-miR-499 or PEG-miR-499 (2.0 mg/kg as miR-499) on day 14 after the implantation. Twenty-four hours after administration of each sample, the tumor tissues were fixed by reflux flow with 1% paraformaldehyde and embedded in Tissue-Tek® O.C.T. Compound (Sakura Finetek Japan, Tokyo, Japan). Frozen tumor-sections of 10 μm thickness were prepared with a Microm HM 505 E Cryostat (Micro-edge Instruments, Tokyo, Japan) and mounted on MAS-coated slides (Matsunami Glass, Osaka, Japan). After having been blocked with 3% BSA in PBS, these tumor sections were incubated with biotinylated anti-mouse CD31 rat monoclonal antibody (BD Biosciences) for 2 h in a humid chamber, and then with streptavidin-Alexa Fluor® 488 conjugate (Life Technologies) for 1 h. The fluorescence of TAMRA-miR-499-C and Alexa Fluor® 488-labeled CD31 was observed under an LSM 510 META confocal microscope (Carl Zeiss, Oberkochen, Germany).

2.11. Knockdown of proteins targeted by miR-499 and VEGF in vivo

The tumor-bearing mice were prepared and injected with APRPG-modified miCont-C/TEPA-PCL (APRPG-miCont) or APRPG-miR-499 (2.0 mg/kg as miRNA) on day 7 after the implantation. The mice were sacrificed under deep anesthesia at 72 h after administration of each sample, and the tumor tissues were excised. Total proteins in the tumors were extracted with Tissue-Protein Extraction Reagent (Pierce) after homogenization with ShakeMan 2 (Biomedical Science, Tokyo, Japan). The expression of proteins targeted by miR-499 (FZD8 and CnAα) and VEGF was examined by Western blotting.

2.12. Therapeutic experiment

The tumor-bearing mice were prepared and injected with APRPG-miR-499 (0.5, 1.0, or 2.0 mg/kg as miR-499) or APRPG-miCont (2.0 mg/kg as miCont) intravenously on days 6 and 9 after implantation of the cells. The tumor size and body weight of each mouse were monitored daily from day 4. Tumor volume was calculated from the following formula: $0.4 \times a \times b^2$ (a; largest diameter, b; smallest diameter).

2.13. Statistical analysis

Differences in a group were evaluated by analysis of variance (ANOVA) with the Tukey's *post-hoc* test.

3. Results

3.1. Characteristics of miR-499 lipoplexes

The chemical structure of DCP-TEPA is presented in Fig. 1A, and the scheme for preparation of miR-499-C/TEPA-PCL and APRPG-miR-499 is shown in Fig. 1B. In this study, miR-499-C/TEPA-PCL were used for *in vitro* experiments; and APRPG-miR-499, for *in vivo* animal experiments. TEM images of TEPA-PCL, miR-499-C/TEPA-PCL, and APRPG-miR-499 are shown in Fig. 1C, D, and E, respectively. miR-499-C/TEPA-PCL were heterogeneous in size. In contrast, APRPG-miR-499 formed uniform-sized circular particles. The particle size and ζ-potential of TEPA-PCL, miR-499-C/TEPA-PCL, PEG-miR-499, and APRPG-miR-499 are shown in Table 1. TEPA-PCL and miR-499-C/TEPA-PCL formed positively-charged nano-vesicles. In contrast, PEG-miR-499 and APRPG-miR-499 showed almost neutral charges and small particle sizes compared with miR-499-C/TEPA-PCL.

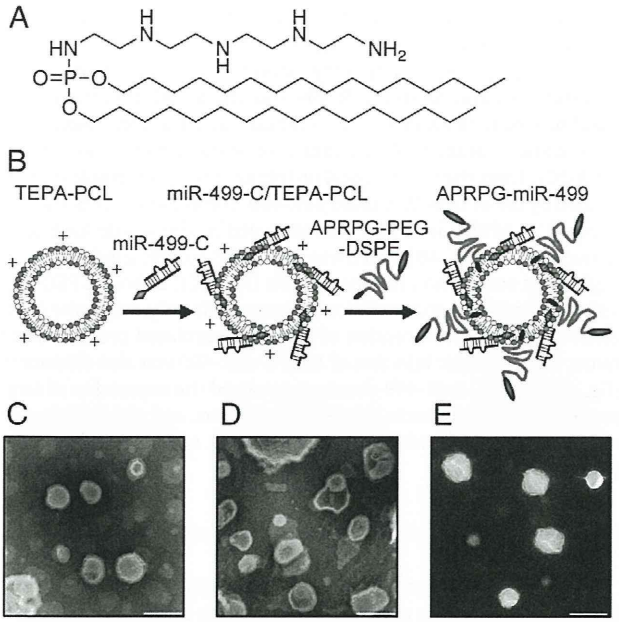

Fig. 1. Preparation and characteristics of TEPA-PCL, miR-499-C/TEPA-PCL, and APRPG-miR-499. (A) Chemical structure of DCP-TEPA, the main lipid component of TEPA-PCL, is shown. (B) Preparation of APRPG-miR-499 is indicated. TEPA-PCL and miR-499-C were mixed to form miR-499-C/TEPA-PCL lipoplexes, which were then incubated with APRPG-PEG-DSPE to prepare APRPG-miR-499. (C–E) TEM images of TEPA-PCL (C), miR-499-C/TEPA-PCL (D), and APRPG-miR-499 (E) are shown. Each sample was negatively-stained with 1% (w/v) ammonium molybdate and observed by TEM. Scale bars indicate 200 nm.

3.2. Anti-angiogenic effects on HUVECs transfected with miR-499-C/TEPA-PCL

The gene-silencing effect of miR-499-C/TEPA-PCL after transfection of HUVECs with these lipoplexes was evaluated *in vitro*. The expression of CnAα, a target protein of miR-499, was repressed after transfection with miR-499-C/TEPA-PCL (100 nM as miR-499) under both hypoxia and normoxia (Fig. 2A). In addition, transfection with a double-dose of miR-499-C/TEPA-PCL (200 nM as miR-499) had a higher knockdown effect under the condition of hypoxia (Fig. 2B). Next, the ability of HUVECs to form capillary-tube networks was assessed after transfection of the cells with miR-499-C/TEPA-PCL. As a result, the networks of capillary tubes were impaired by miR-499-C/TEPA-PCL under both hypoxia and normoxia (Fig. 2C), and the tube length formed by the transfected-HUVECs was significantly shorter in the miR-499-C/TEPA-PCL group than in the control group (Fig. 2D). Especially, under the condition of hypoxia, miR-499 induced stronger inhibition of tube networks than that under normoxia. Growth inhibition of HUVECs after the transfection with miR-499 was also evaluated. The result showed that growth of HUVECs at 48 h after the start of the transfection was significantly inhibited by miR-499-C/TEPA-PCL under both hypoxia and normoxia (Fig. 2E).

Table 1
Characteristics of TEPA-PCL, miR-499-C/TEPA-PCL, PEG-miR-499, and APRPG-miR-499.

	Size (d·nm)	PdI	ζ-Potential (mV)
TEPA-PCL	136.1 ± 13.0	0.153 ± 0.060	+50.3 ± 4.4
miR-499-C/TEPA-PCL	200.2 ± 27.3	0.256 ± 0.088	+47.0 ± 2.1
PEG-miR-499	157.0 ± 13.1	0.199 ± 0.030	−1.9 ± 1.1
APRPG-miR-499	177.1 ± 22.1	0.215 ± 0.041	−1.6 ± 0.7

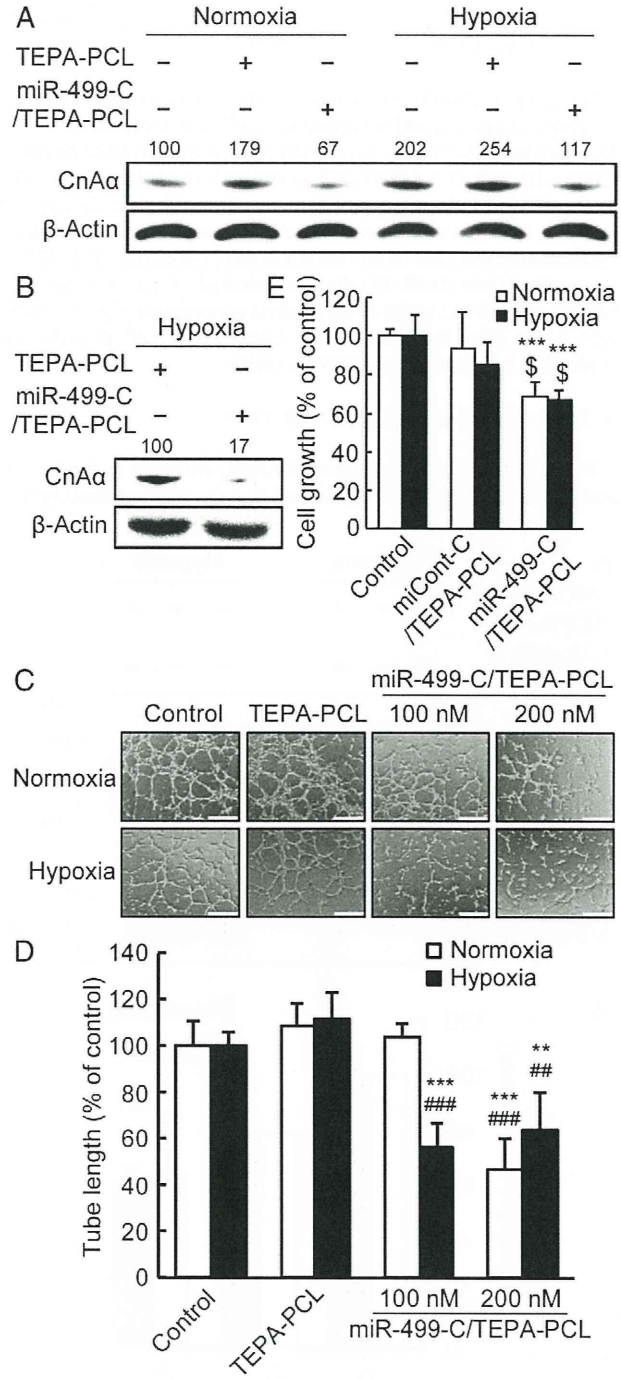

Fig. 2. Antiangiogenic effects on HUVECs transfected with miR-499 were evaluated under the conditions of hypoxia and normoxia. (A, B) The expression of CnAα at 48 h after transfection with TEPA-PCL or miR-499-C/TEPA-PCL at an miR-499 concentration of 100 nM (A) or 200 nM (B) was examined by Western blotting. The values are presented as the percentage of density (A; *vs.* control under normoxia, B; *vs.* TEPA-PCL under hypoxia). (C, D) Capillary tube networks formed by the HUVECs transfected with TEPA-PCL; miR-499-C/TEPA-PCL at 100 nM as miR-499 or that at 200 nM for 48 h were observed under a microscope (C), and the tube length of these was measured (D). Scale bars indicate 100 μm. The data on tube length is presented as a percentage (with SD bars) of that in the control group under the same culture conditions. The symbols show significant differences (***P < 0.001, **P < 0.01 *vs.* control, ###P < 0.001, ##P < 0.01 *vs.* TEPA-PCL). (E) Growth of HUVECs at 48 h after transfection with miCont-C/TEPA-PCL or miR-499-C/TEPA-PCL (100 nM as miRNA) was assessed. Data are presented as a percentage (with SD bars) of growth in the control group under the same culture conditions. The symbols show significant differences (***P < 0.001 *vs.* control, $^{\$}P$ < 0.05 *vs.* miCont-C/TEPA-PCL).

3.3. Inhibition of VEGF secretion and of cell proliferation of Colon 26 NL-17 cells by transfection with miR-499-C/TEPA-PCL

Secretion of VEGF from the cancer cells was examined under the conditions of hypoxia and normoxia (Fig. 3A). The secretion of mouse VEGF variants including VEGF164 and VEGF120 was inhibited by transfection with miR-499-C/TEPA-PCL under both conditions. Especially, drastic miR-499-induced suppression was observed under the hypoxic condition; although VEGF in the control group was elevated under hypoxia compared with that under normoxia. Next, the effect of miR-499 on the growth of Colon 26 NL-17 cells was evaluated after transfection with miR-499-C/TEPA-PCL under either hypoxia or normoxia (Fig. 3B). Forty-eight hours after the start of the transfection, cell growth was significantly inhibited under either condition.

3.4. Tumor-targeted delivery of miR-499 in vivo

To evaluate the biodistribution of APRPG-miR-499 in the tumor-bearing mice, we injected [^{3}H]-labeled lipoplexes intravenously into the mice. Twenty-four hours later, the biodistribution of each type of lipoplex was examined (Fig. 4A). TEPA-PCL were detected mainly in the liver and spleen, but not in the blood or tumor. On the other hand, PEG-miR-499 and APRPG-miR-499 showed a high retention in the blood plasma with avoidance of accumulation in the liver. Additionally, these particles dramatically accumulated in the tumor compared with TEPA-PCL. Then, the intratumoral distribution of these samples was examined by use of TAMRA-labeled miR-499. The fluorescence of miR-499 injected as APRPG-miR-499 was observed in the whole area of the tumor sections (Fig. 4B), and these lipoplexes accumulated in both the angiogenic vessels and the tumor cells (Fig. 4C); although PEG-miR-499 exhibited local accumulation in tumor cells only, not in the angiogenic vessels. The expression of miR-499-regulated proteins in the tumor after systemic injection of APRPG-miR-499 was also determined (Fig. 4D). APRPG-miR-499 clearly suppressed the expression of target proteins of miR-499, including FZD8 and CnAα, and also inhibited the expression of VEGF, which is regulated by a series of such targeted proteins.

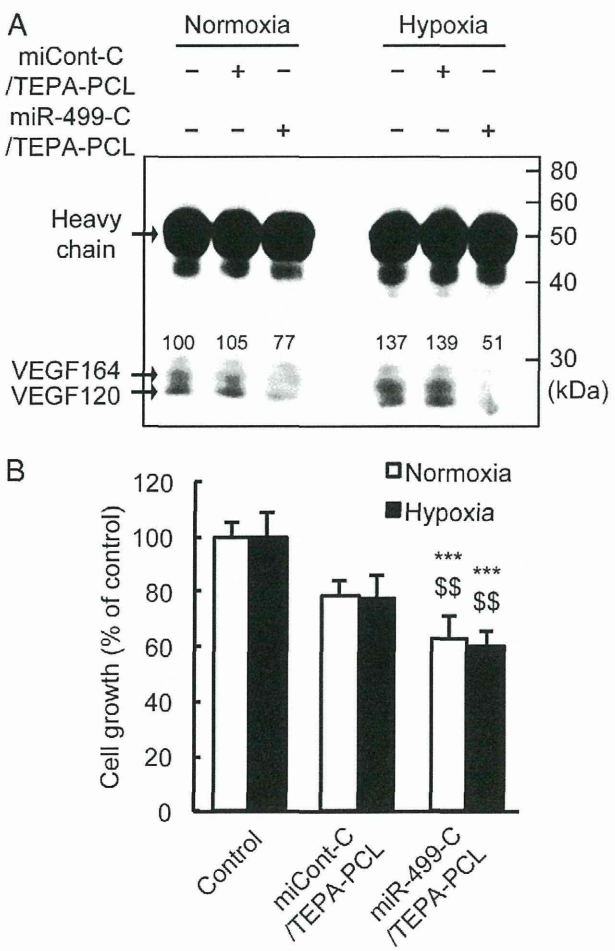

Fig. 3. Antiangiogenic and antiproliferative effects on Colon 26 NL-17 cells transfected with miR-499 were evaluated under hypoxia or normoxia. (A) The secretion of VEGF into the media conditioned by Colon 26 NL-17 cells transfected with miCont-C/TEPA-PCL or miR-499-C/TEPA-PCL (100 nM as miRNA) for 48 h was examined by immunoprecipitation/Western blotting. The conditioned media applied to immunoprecipitation were corrected with total protein content of the cells before the assay. The values are presented as the percentage of density (*vs.* control under normoxia). (B) Growth of Colon 26 NL-17 cells at 48 h after transfection with miCont-C/TEPA-PCL or miR-499-C/TEPA-PCL was assessed. Data are presented as the percentage (with SD bars) of the growth in the control group under the same culture conditions. The symbols show significant differences (***$P < 0.001$ *vs.* control, $^{\$\$}P < 0.01$ *vs.* miCont-C/TEPA-PCL).

3.5. Therapeutic effect of miR-499 on tumor growth

APRPG-miR-499 was intravenously administered to the tumor-bearing mice at a dose of 0.5, 1.0 or 2.0 mg/kg as miR-499. The result showed that all 3 doses of APRPG-miR-499 gave almost the same level of tumor-growth inhibition (Fig. 5A). APRPG-miR-499 significantly inhibited the tumor growth compared with the control or APRPG-miCont (Fig. 5B). Body weight of the treated-mice was not changed among all groups (Fig. 5C). It appeared that APRPG-miR-499 had a potentially therapeutic effect on tumor growth even at the low dose of 0.5 mg/kg as miR-499.

4. Discussion

For effective treatment of cancer, therapeutic agents should be effective under the hypoxic condition [29–31]. Thus, we evaluated the gene-silencing effect of miR-499 under both hypoxia and normoxia *in vitro*. miR-499 has various kinds of target genes and regulates a series of signaling pathways [13,32–34]. CnAα is one of the proteins targeted by miR-499 and is reported to be over-expressed under the hypoxic or ischemic condition [12]. In fact, our data indicated that the expression of CnAα mRNA in HUVECs increased under hypoxia (Supplementary Fig. S1A) and that the protein expression of CnAα also increased under this condition (Supplementary Fig. S1B). miR-499 induced effective knockdown of CnAα expression and had significant antiangiogenic effects under both hypoxia and normoxia (Fig. 2). In addition, as was shown in Fig. 2C and D, the antiangiogenic effect of miR-499 was stronger under hypoxia. Since the uptake of the miR-499 lipoplexes was not affected by the condition of hypoxia (Supplementary Fig. S2), this enhanced antiangiogenic effect was not ascribable to alteration of the amount of miR-499 that entered the cells. Under the present experimental condition, significant cell death induced by hypoxia was not observed. We speculate that this difference in efficacy might have been caused by specific roles of miR-499 under hypoxia as mentioned above, although the mechanism remains unclear.

Our data showed that miR-499 suppressed VEGF secretion from Colon 26 NL-17 cells under both hypoxia and normoxia and that this suppression was especially remarkable under hypoxia (Fig. 3A). Since a decrease in VEGF activity is effectively antiangiogenic [35–37], it would appear that miR-499 induced integrative antiangiogenic effects by its delivery to not only angiogenic endothelial cells but also cancer cells to inhibit their secretion of VEGF. In addition, miR-499 directly inhibited the growth of cancer cells (Fig. 3B). These results suggest that miR-499 had a potent therapeutic effect on tumor growth *via* the integrative antiangiogenic effects and the direct inhibition of cancer cell growth.

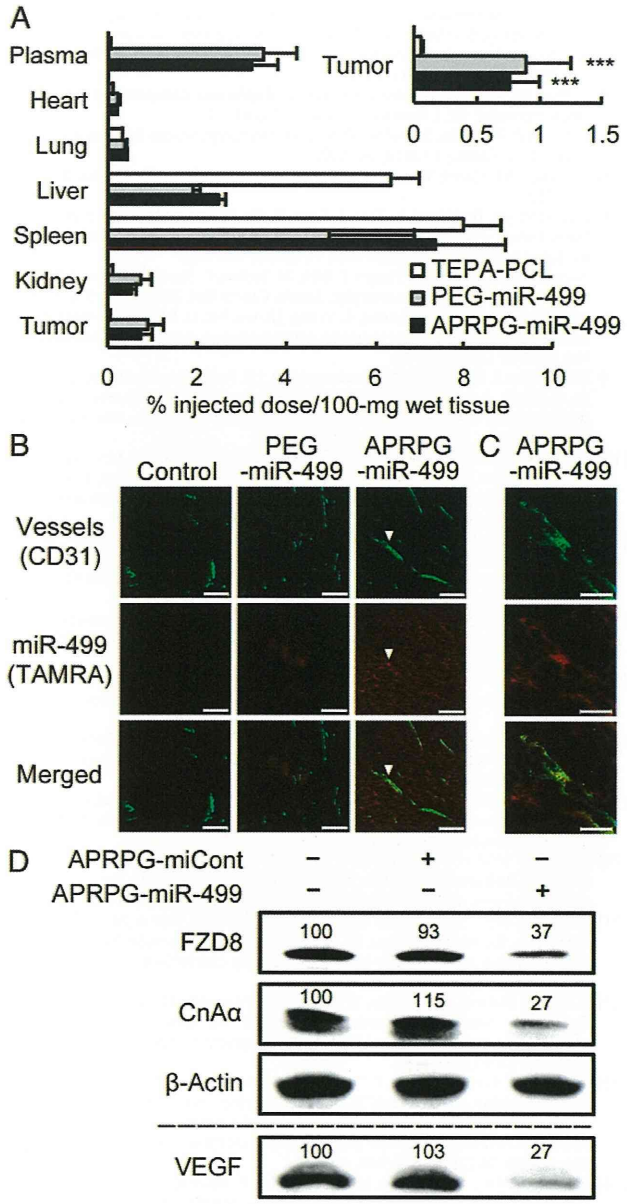

Fig. 4. *In vivo* delivery of miR-499 *via* systemic administration and its gene-silencing effects on the tumor were evaluated. (A) Biodistribution of APRPG-miR-499 in the tumor-bearing mice was determined. BALB/c mice bearing Colon 26 NL-17 cells (n = 6) were injected with [^{3}H]-labeled TEPA-PCL as TEPA-PCL alone, PEG-miR-499 or APRPG-miR-499 (74 kBq/mouse, 1.0 mg/kg as miR-499) *via* a tail vein. Twenty-four hours after the injection, radioactivity in each organ was counted with a liquid scintillation counter. Data are presented as the percentage (with SD bars) of the injected dose per 100-mg wet tissue. Asterisks show significant differences (***$P < 0.001$ *vs.* TEPA-PCL). (B, C) Intratumoral distribution of miR-499 at low magnification (B) and at high magnification of the area indicated by the arrowheads in "B" (C) was examined. The tumor-bearing mice were injected with TAMRA-labeled miR-499 carried as PEG-miR-499 or APRPG-miR-499 (2.0 mg/kg as miRNA), and frozen-tumor sections at 10-μm thickness were prepared at 24 h after the injection. CD31 was immunostained, and the intratumoral distribution of TAMRA-miR-499 was observed by confocal laser-scanning microscopy. Scale bars indicate 100 μm and 20 μm in panels B and C, respectively. (D) The expression of proteins targeted by miR-499 (FZD8 and CnAα) and of VEGF in the tumor tissues was examined by Western blotting. The tumor-bearing mice were intravenously injected with APRPG-miCont or APRPG-miR-499 (2.0 mg/kg as miRNA), and the tumors were excised at 72 h after the injection. Total proteins of the tumors were extracted, and the expression of FZD8, CnAα, and VEGF was determined. The values are presented as the percentage of density (*vs.* control in each protein examined).

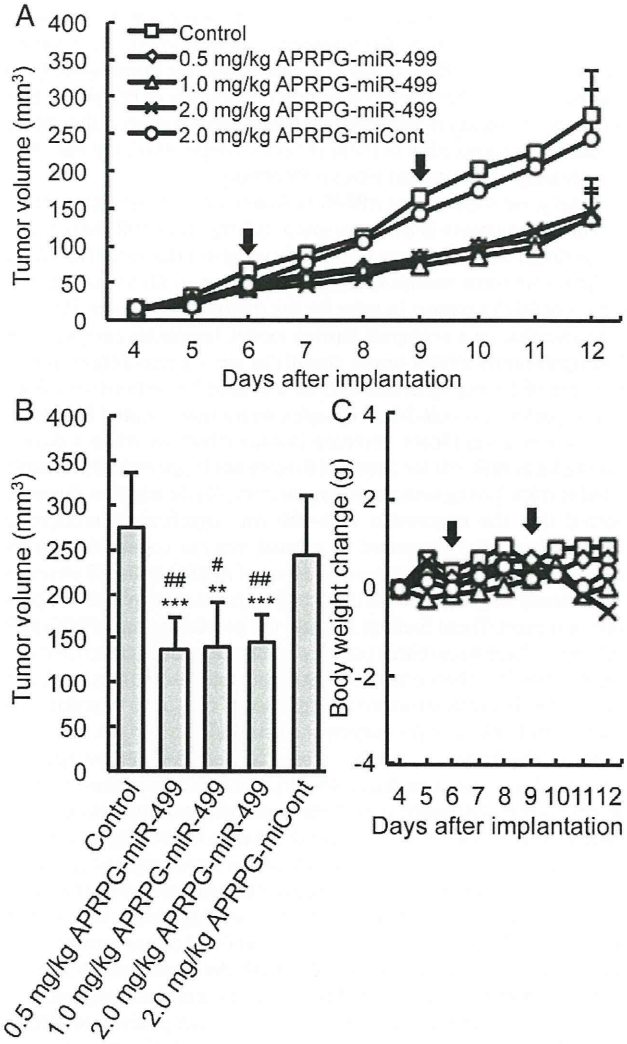

Fig. 5. Therapeutic effect of APRPG-miR-499 on tumor growth was examined. (A) Tumor-bearing mice (n = 6) were injected with APRPG-miR-499 at a dose of 0.5, 1.0 or 2.0 mg/kg as miR-499 or APRPG-miCont (2.0 mg/kg as miCont) *via* a tail vein on days 6 and 9 (indicated by arrows) after the implantation. Data indicate the tumor volume from days 4 to 12. (B) Data from day 12 in "A" as a bar graph. (C) Change in body weight of the mice. Data are presented as the mean of the tumor volume or the body weight change with SD bars. Symbols indicate significant differences (***$P < 0.001$, **$P < 0.01$ *vs.* control, ##$P < 0.01$, #$P < 0.05$ *vs.* APRPG-miCont).

For intravenous targeted delivery of miR-499 to tumors, APRPG-grafted PEG was used to modify the surface of miR-499 lipoplexes. APRPG has an affinity for VEGF receptor-1 (VEGFR1), which is known to be over-expressed on angiogenic endothelial cells in tumors [38]. Additionally, VEGFR1 is also highly expressed on certain kinds of cancer cells, including Colon 26 NL-17 carcinoma cells (Supplementary Fig. S3). Therefore, miR-499 should be intravenously delivered to both angiogenic endothelial cells and cancer cells by modification with APRPG-PEG. In addition, targeted delivery with APRPG-PEG may contribute to prevent unanticipated effects of miR-499 on normal tissues, although there are few reports showing the toxicity of miR-499. The accumulation of APRPG-miR-499 was observed in both angiogenic vessels and cancer cells, although PEG-miR-499 lipoplexes were detected only in the cancer cells (Fig. 4B). However, the amount of APRPG-miR-499 accumulated in the entire tumor was almost the same as that of PEG-miR-499 (Fig. 4A). We previously obtained similar results showing that APRPG modification improves the intratumoral distribution but not the amount accumulated in tumors in the case of PEGylated

liposomes [39]. In addition, anticancer effects of therapeutic siRNA formulated in PEGylated lipoplexes were significantly improved by surface modification with APRPG in mice bearing melanoma tumors [40]. These findings suggest that the intratumoral distribution of PEGylated liposomes or lipoplexes is improved by ligand modification, although the amount of accumulation of them in tumors depends on the enhanced permeability and retention effect (EPR effect).

Finally, we showed that APRPG-miR-499 induced significant inhibition of tumor growth at a dose as low as 0.5 mg/kg as miR-499 (total of 2 injections) with no change in the body weight of the mice (Fig. 5A and B). There are some studies in which a certain microRNA was delivered intravenously to tumors in mice for the treatment of cancer. Wu et al. indicated that, in a xenograft murine model, lipoplexes carrying miR-29b significantly inhibit tumor growth by intravenous administration at a dose of 1.5 mg/kg as miR-29b for a total of 7 injections [41]. Trang et al. reported that miR-34a in complex with a novel neutral lipid emulsion causes a significant decrease in tumor burden when a dose of 1.0 mg/kg as miR-34a for a total of 8 injections is systemically administered to mice having orthotopic lung tumors [42]. In addition, it was reported that the expression miR-499 was significantly reduced in colorectal cancers compared to normal mucosa collected from the same patients [43]. The anticancer effect of APRPG-miR-499 observed in this study might be related to such dysregulation of miR-499 expression in tumors. These findings indicate the possibility that APRPG-miR-499 would have an excellent potency as a therapeutic agent to treat cancer. It is reported that certain antiangiogenic agents can transiently normalize the abnormal structure and function of the tumor vasculature to make it more efficient for oxygen and drug delivery [44]. In fact, many types of antiangiogenic agents are used for combination therapy with other kinds of anticancer drugs [45–49]. Since the antiangiogenic effect of APRPG-miR-499 might contribute to vascular normalization, combination therapy of it with anticancer drugs is an interesting approach.

In conclusion, APRPG-miR-499 lipoplexes were prepared for *in vivo* delivery of miR-499; and they effectively accumulated in the tumor *via* systemic administration to tumor-bearing mice. In addition, APRPG-miR-499 induced significant inhibition of tumor growth when used at a quite low dose of miR-499 with the consequence of being knockdown of proteins targeted by it. Our present study suggests that the tumor-targeted delivery of miR-499 has high potency to achieve microRNA-based cancer therapy *via* intravenous administration.

Supplementary data to this article can be found online at http://dx.doi.org/10.1016/j.jconrel.2014.02.019.

Disclosure of potential conflicts of interest

No potential conflicts of interest were disclosed.

Acknowledgments

This research was supported by a grant-in-aid for scientific research from the Japan Society for the Promotion of Science.

References

[1] A. Lujambio, S.W. Lowe, The microcosmos of cancer, Nature 482 (2012) 347–355.
[2] K.J. Png, N. Halberg, M. Yoshida, S.F. Tavazoie, A microRNA regulon that mediates endothelial recruitment and metastasis by cancer cells, Nature 481 (2012) 190–194.
[3] M.S. Zaman, V. Shahryari, G. Deng, S. Thamminana, S. Saini, S. Majid, I. Chang, H. Hirata, K. Ueno, S. Yamamura, K. Singh, Y. Tanaka, Z.L. Tabatabai, R. Dahiya, Up-regulation of microRNA-21 correlates with lower kidney cancer survival, PLoS One 7 (2012) e31060.
[4] S. Yoshizawa, J.H. Ohyashiki, M. Ohyashiki, T. Umezu, K. Suzuki, A. Inagaki, S. Iida, K. Ohyashiki, Downregulated plasma miR-92a levels have clinical impact on multiple myeloma and related disorders, Blood Cancer J. 2 (2012) e53.
[5] N. Xu, L. Zhang, F. Meisgen, M. Harada, J. Heilborn, B. Homey, D. Grander, M. Stahle, E. Sonkoly, A. Pivarcsi, MicroRNA-125b down-regulates matrix metallopeptidase 13 and inhibits cutaneous squamous cell carcinoma cell proliferation, migration, and invasion, J. Biol. Chem. 287 (2012) 29899–29908.
[6] N.M. Alajez, M. Lenarduzzi, E. Ito, A.B.Y. Hui, W. Shi, J. Bruce, S.J. Yue, S.H. Huang, W. Xu, J. Waldron, B. O'Sullivan, F.F. Liu, miR-218 suppresses nasopharyngeal cancer progression through downregulation of survivin and the SLIT2–ROBO1 pathway, Cancer Res. 71 (2011) 2381–2391.
[7] G. Zhao, B.L. Rodriguez, Molecular targeting of liposomal nanoparticles to tumor microenvironment, Int. J. Nanomedicine 8 (2013) 61–71.
[8] L. Zhu, V.P. Torchilin, Stimulus-responsive nanopreparations for tumor targeting, Integr. Biol. (Camb.) 5 (2013) 96–107.
[9] M. Halasi, A.L. Gartel, Targeting FOXM1 in cancer, Biochem. Pharmacol. 85 (2013) 644–652.
[10] L. Li, R. Wang, D. Wilcox, X. Zhao, J. Song, X. Lin, W.M. Kohlbrenner, S.W. Fesik, Y. Shen, Tumor vasculature is a key determinant for the efficiency of nanoparticle-mediated siRNA delivery, Gene Ther. 19 (2012) 775–780.
[11] V. Catalano, A. Turdo, S. Di Franco, F. Dieli, M. Todaro, G. Stassi, Tumor and its microenvironment: a synergistic interplay, Semin. Cancer Biol. 23P (2013) 522–532.
[12] J.X. Wang, J.Q. Jiao, Q. Li, B. Long, K. Wang, J.P. Liu, Y.R. Li, P.F. Li, miR-499 regulates mitochondrial dynamics by targeting calcineurin and dynamin-related protein-1, Nat. Med. 17 (2011) 71–78.
[13] K.D. Wilson, S. Hu, S. Venkatasubrahmanyam, J.D. Fu, N. Sun, O.J. Abilez, J.J. Baugh, F. Jia, Z. Ghosh, R.A. Li, A.J. Butte, J.C. Wu, Dynamic microRNA expression programs during cardiac differentiation of human embryonic stem cells: role for miR-499, Circ. Cardiovasc. Genet. 3 (2010) 426–435.
[14] K.H. Baek, A. Zaslavsky, R.C. Lynch, C. Britt, Y. Okada, R.J. Siarey, M.W. Lensch, I.H. Park, S.S. Yoon, T. Minami, J.R. Korenberg, J. Folkman, G.Q. Daley, W.C. Aird, Z. Galdzicki, S. Ryeom, Down's syndrome suppression of tumor growth and the role of the calcineurin inhibitor DSCR1, Nature 459 (2009) 1126–1130.
[15] A. Courtwright, S. Siamakpour-Reihani, J.L. Arbiser, N. Banet, E. Hilliard, L. Fried, C. Livasy, D. Ketelsen, D.B. Nepal, C.M. Perou, C. Patterson, N. Klauber-DeMore, Secreted frizzle-related protein 2 stimulates angiogenesis via a calcineurin/NFAT signaling pathway, Cancer Res. 69 (2009) 4621–4628.
[16] A.W. Drzewiecka, M. Ratajewski, W. Wagner, J. Dastych, HIF-1α is up-regulated in activated mast cells by a process that involves calcineurin and NFAT, J. Immunol. 181 (2008) 1665–1672.
[17] X. Zhang, J.P. Gaspard, D.C. Chung, Regulation of vascular endothelial growth factor by the Wnt and K-ras pathways in colonic neoplasia, Cancer Res. 61 (2001) 6050–6054.
[18] S. Huang, K. Shao, Y. Liu, Y. Kuang, J. Li, S. An, Y. Guo, H. Ma, C. Jiang, Tumor-targeting and microenvironment-responsive smart nanoparticles for combination therapy of antiangiogenesis and apoptosis, ACS Nano 7 (2013) 2860–2871.
[19] V. Perotti, P. Baldassari, I. Bersani, A. Molla, C. Vegetti, E. Tassi, J. Dal Col, R. Dolcetti, A. Anichini, R. Mortarini, NFATc2 is a potential therapeutic target in human melanoma, J. Invest. Dermatol. 132 (2012) 2652–2660.
[20] E.M. Gallo, M.M. Winslow, K. Cante-Barrett, A.N. Radermacher, L. Ho, L. McGinnis, B. Iritani, J.R. Neilson, G.R. Crabtree, Calcineurin sets the bandwidth for discrimination of signals during thymocyte development, Nature 450 (2007) 731–735.
[21] Y. Pei, S.N. Brun, S.L. Markant, W. Lento, P. Gibson, M.M. Taketo, M. Giovannini, R.J. Gilbertson, R.J. Wechsler-Reya, WNT signaling increases proliferation and impairs differentiation of stem cells in the developing cerebellum, Development 139 (2012) 1724–1733.
[22] T. Asai, S. Matsushita, E. Kenjo, T. Tsuzuku, N. Yonenaga, H. Koide, K. Hatanaka, T. Dewa, M. Nango, N. Maeda, H. Kikuchi, N. Oku, Dicetyl phosphate-tetraethylenepentamine-based liposomes for systemic siRNA delivery, Bioconjug. Chem. 22 (2011) 429–435.
[23] H. Koide, T. Asai, K. Furuya, T. Tsuzuku, H. Kato, T. Dewa, M. Nango, N. Maeda, N. Oku, Inhibition of Akt (ser473) phosphorylation and rapamycin-resistant cell growth by knockdown of mammalian target of rapamycin with small interfering RNA in vascular endothelial growth factor receptor-1-targeting vector, Biol. Pharm. Bull. 34 (2011) 602–608.
[24] E. Kenjo, T. Asai, N. Yonenaga, H. Ando, T. Ishii, K. Hatanaka, K. Shimizu, Y. Urita, T. Dewa, M. Nango, H. Tsukada, N. Oku, Systemic delivery of small interfering RNA by use of targeted polycation liposomes for cancer therapy, Biol. Pharm. Bull. 36 (2013) 287–291.
[25] N. Yonenaga, E. Kenjo, T. Asai, A. Tsuruta, K. Shimizu, T. Dewa, M. Nango, N. Oku, RGD-based active targeting of novel polycation liposomes bearing siRNA for cancer treatment, J. Control. Release 160 (2012) 177–181.
[26] H. Ando, A. Okamoto, M. Yokota, K. Shimizu, T. Asai, T. Dewa, N. Oku, Development of a miR-92a delivery system for anti-angiogenesis-based cancer therapy, J. Gene Med. 15 (2013) 20–27.
[27] H. Ando, A. Okamoto, M. Yokota, T. Asai, T. Dewa, N. Oku, Polycation liposomes as a vector for potential intracellular delivery of microRNA, J. Gene Med. 15 (2013) 375–383.
[28] N. Oku, K. Doi, Y. Namba, S. Okada, Therapeutic effect of adriamycin encapsulated in long-circulating liposomes on Meth-A-sarcoma-bearing mice, Int. J. Cancer 58 (1994) 415–419.
[29] A.K. Iyer, A. Singh, S. Ganta, M.M. Amiji, Role of integrated cancer nanomedicine in overcoming drug resistance, Adv. Drug Deliv. Rev. 65 (2013) 1784–1802.
[30] Y. Huang, S. Goel, D.G. Duda, D. Fukumura, R.K. Jain, Vascular normalization as an emerging strategy to enhance cancer immunotherapy, Cancer Res. 73 (2013) 2943–2948.
[31] T.R. Spivak-Kroizman, G. Hostetter, R. Posner, M. Aziz, C. Hu, M.J. Demeure, D. Von Hoff, S.R. Hingorani, T.B. Palculict, J. Izzo, G.M. Kiriakova, M. Abdelmelek, G. Bartholomeusz, B.P. James, G. Powis, Hypoxia triggers hedgehog-mediated tumor-stromal interactions in pancreatic cancer, Cancer Res. 73 (2013) 3235–3247.
[32] X.Q. Liu, Z.Y. Zhang, L. Sun, N. Chai, S.H. Tang, J. Jin, H. Hu, Y.Z. Nie, X. Wang, K.C. Wu, H.F. Jin, D.M. Fan, MicroRNA-499-5p promotes cellular invasion and tumor

metastasis in colorectal cancer by targeting FOXO4 and PDCD4, Carcinogenesis 32 (2011) 1798–1805.
[33] J.T.C. Shieh, Y. Huang, J. Gilmore, D. Srivastava, Elevated miR-499 levels blunt the cardiac stress response, PLoS One 6 (2011) e19481.
[34] J.D. Fu, S.N. Rushing, D.K. Lieu, C.W. Chan, C.W. Kong, L. Geng, K.D. Wilson, N. Chiamvimonvat, K.R. Boheler, J.C. Wu, G. Keller, R.J. Hajjar, R.A. Li, Distinct roles of microRNA-1 and -499 in ventricular specification and functional maturation of human embryonic stem cell-derived cardiomyocytes, PLoS One 6 (2011) e27417.
[35] Y. Zhang, N.M. Schwerbrock, A.B. Rogers, W.Y. Kim, L. Huang, Codelivery of VEGF siRNA and gemcitabine monophosphate in a single nanoparticle formulation for effective treatment of NSCLC, Mol. Ther. 21 (2013) 1559–1569.
[36] S.H. Lee, J. Lee, M.H. Jung, Y.M. Lee, Glyceollins, a novel class of soy phytoalexins, inhibit angiogenesis by blocking the VEGF and bFGF signaling pathways, Mol. Nutr. Food Res. 57 (2013) 225–234.
[37] J. Xu, J. Wang, B. Xu, H. Ge, X. Zhou, J.Y. Fang, Colorectal cancer cells refractory to anti-VEGF treatment are vulnerable to glycolytic blockade due to persistent impairment of mitochondria, Mol. Cancer Ther. 12 (2013) 717–724.
[38] M. Talagas, A. Uguen, R. Garlantezec, G. Fournier, L. Doucet, E. Gobin, P. Marcorelles, A. Volant, M. DE Braekeleer, VEGFR1 and NRP1 endothelial expressions predict distant relapse after radical prostatectomy in clinically localized prostate cancer, Anticancer Res. 33 (2013) 2065–2075.
[39] Y. Murase, T. Asai, Y. Katanasaka, T. Sugiyama, K. Shimizu, N. Maeda, N. Oku, A novel DDS strategy, "dual-targeting", and its application for antineovascular therapy, Cancer Lett. 287 (2010) 165–171.
[40] H. Koide, T. Asai, H. Kato, N. Yonenaga, H. Ando, T. Dewa, M. Nango, N. Maeda, N. Oku, Susceptibility of PTEN-positive Metastatic Tumors to Small Interfering RNA Targeting the Mammalian Target of Rapamycin, 2014. (submitted for publication).
[41] Y. Wu, M. Crawford, Y. Mao, R.J. Lee, I.C. Davis, T.S. Elton, L.J. Lee, S.P. Nana-Sinkam, Therapeutic delivery of microRNA-29b by cationic lipoplexes for lung cancer, Mol. Ther. Nucleic Acids 2 (2013) e84.
[42] P. Trang, J.F. Wiggins, C.L. Daige, C. Cho, M. Omotola, D. Brown, J.B. Weidhaas, A.G. Bader, F.J. Slack, Systemic delivery of tumor suppressor microRNA mimics using a neutral lipid emulsion inhibits lung tumors in mice, Mol. Ther. 19 (2011) 1116–1122.
[43] S. Vinci, S. Gelmini, I. Mancini, F. Malentacchi, M. Pazzagli, C. Beltrami, P. Pinzani, C. Orlando, Genetic and epigenetic factors in regulation of microRNA in colorectal cancers, Methods 59 (2013) 138–146.
[44] R.K. Jain, Normalization of tumor vasculature: an emerging concept in antiangiogenic therapy, Science 307 (2005) 58–62.
[45] N. Cheng, T. Xia, Y. Han, Q.J. He, R. Zhao, J.R. Ma, Synergistic antitumor effects of liposomal honokiol combined with cisplatin in colon cancer models, Oncol. Lett. 2 (2011) 957–962.
[46] X.L. Guo, D. Li, K. Sun, J. Wang, Y. Liu, J.R. Song, Q.D. Zhao, S.S. Zhang, W.J. Deng, X. Zhao, M.C. Wu, L.X. Wei, Inhibition of autophagy enhances anticancer effects of bevacizumab in hepatocarcinoma, J. Mol. Med. 91 (2013) 473–483.
[47] K.L. Meadows, H.I. Hurwitz, Anti-VEGF therapies in the clinic, Cold Spring Harb. Perspect. Med. 2 (2012) a006577.
[48] V.P. Chauhan, J.D. Martin, H. Liu, D.A. Lacorre, S.R. Jain, S.V. Kozin, T. Stylianopoulos, A.S. Mousa, X. Han, P. Adstamongkonkul, Z. Popovic, P. Huang, M.G. Bawendi, Y. Boucher, R.K. Jain, Angiotensin inhibition enhances drug delivery and potentiates chemotherapy by decompressing tumour blood vessels, Nat. Commun. 4 (2013) 2516.
[49] B. Diop-Frimpong, V.P. Chauhan, S. Krane, Y. Boucher, R.K. Jain, Losartan inhibits collagen I synthesis and improves the distribution and efficacy of nanotherapeutics in tumors, Proc. Natl. Acad. Sci. U. S. A. 108 (2011) 2909–2914.

Cardiovasc Drugs Ther (2012) 26:409–416
DOI 10.1007/s10557-012-6410-4

Design and Rationale of Low-Dose Erythropoietin in Patients with ST-Segment Elevation Myocardial Infarction (EPO-AMI-II Study): A Randomized Controlled Clinical Trial

Tetsuo Minamino · Ken Toba · Shuichiro Higo · Daisaku Nakatani · Shungo Hikoso · Masao Umegaki · Kouji Yamamoto · Yoshiki Sawa · Yoshifusa Aizawa · Issei Komuro · EPO-AMI-II study investigators

Published online: 2 September 2012

Abstract
Purpose The development of novel pharmaceutical interventions to improve the clinical outcomes of patients with acute ST-segment elevation myocardial infarction (STEMI) is an unmet medical need worldwide. In animal models, a single intravenous administration of erythropoietin (EPO) during reperfusion improves left ventricular (LV) function in the chronic stage. However, the results of recent proof-of-concept trials using high-dose EPO in patients with STEMI are inconsistent. In our pilot study, low-dose EPO after successful percutaneous coronary intervention (PCI) improved the LV ejection fraction (EF) and did not trigger severe adverse clinical events in patients with STEMI. One possible reason for this discrepancy is the dose of EPO used.
Methods and results We have started a double-blind, placebo-controlled, randomized, multicenter clinical trial (EPO-AMI-II) to clarify the safety and efficacy of low-dose EPO in patients with STEMI. STEMI patients who have a low LVEF (<50 %) will be randomly assigned to intravenous administration of placebo or EPO (6,000 or 12,000 IU) within 6 h after successful PCI. The primary endpoint is the difference in LVEF between the acute and chronic phases (6 months), as measured by single-photon emission computed tomography. The patient number needed for EPO-AMI-II is 600. The study will stop when superior efficacy or futility is detected by an interim analysis. This study has been approved by the Evaluation System of Investigational Medical Care.
Conclusions EPO-AMI-II study will clarify the safety and efficacy of low-dose EPO in STEMI patients with LV dysfunction in a double-blind, placebo-controlled, multicenter study. (247 words)

Key words Erythropoietin · Low-dose · Acute myocardial infarction · LV dysfunction

Names of Grants: Grants-in-Aid from the Ministry of Health, Labour and Welfare (Japan); the Ministry of Education's Support and Training Program for Translational Research at Osaka University; and the Japanese Circulation Society Grant for Translational Research 2010

T. Minamino · S. Higo · D. Nakatani · S. Hikoso · Y. Sawa · I. Komuro (✉)
Department of Cardiovascular Medicine,
Osaka University Graduate School of Medicine,
2-2 Yamada-oka,
Suita, Osaka 565-0871, Japan
e-mail: komuro-tky@umin.ac.jp

K. Yamamoto
Department of Biomedical Statistics,
Osaka University Hospital,
Suita, Japan

M. Umegaki
Medical Center for Translational Research, Osaka University Hospital,
Suita, Japan

K. Toba
First Department of Internal Medicine,
Niigata University Medical and Dental Hospital,
Niigata, Japan

Y. Aizawa
Tachikawa Medical Center,
Nagaoka, Japan

Despite improved clinical outcomes by early reperfusion with thrombolysis and primary percutaneous coronary intervention (PCI) with stenting, the mortality of patients with